ACS Photonics

Article

pubs.acs.org/journal/apchd5

Large-Area Printing of Optical Gratings and 3D Photonic Crystals Using Solution-Processable Nanoparticle/Polymer Composites

Michael R. Beaulieu, Nicholas R. Hendricks, and James J. Watkins*

Center for Hierarchical Manufacturing, Department of Polymer Science and Engineering, University of Massachusetts Amherst, 120 Governors Drive, Amherst, Massachusetts 01003, United States

ABSTRACT: We demonstrate a readily scalable print, lift, and stack approach for producing large-area, 3D photonic crystal (PC) structures and optical gratings. UV-assisted nanoimprint lithography was used to pattern grating structures composed of highly filled nanoparticle (NP) polymer composite resists with tunable refractive indices (RI). The gratings were robust and upon release from a support substrate were oriented and stacked to yield 3D PCs. The composite resists were composed of anatase titania (TiO_2) NPs, between 5 and 30 nm in diameter, and a UV-curable optical resist (Norland Optical Adhesive 60). The RI of the composite resists was tuned between 1.58 and 1.92 at 800 nm while maintaining excellent optical transparency. The grating structure dimensions, line width, depth, and pitch were easily varied by simply changing the imprint mold. A six-layer log-pile stack was prepared using a composite resist containing 50 wt % TiO_2 NPs with an RI of 1.72 and yielded up to 72% reflection at 840 nm and a minimum reflection of 50% over broad angles of incidence (25−65°) and grating areas of >6 cm^2. The grating patterning process is readily scalable for roll-to-roll production, and the ability to tailor RI as well as grating structure dimensions and orientation offers an attractive means for large-area production of tuned optical materials, while automating alignment will enable high-volume production of PCs.

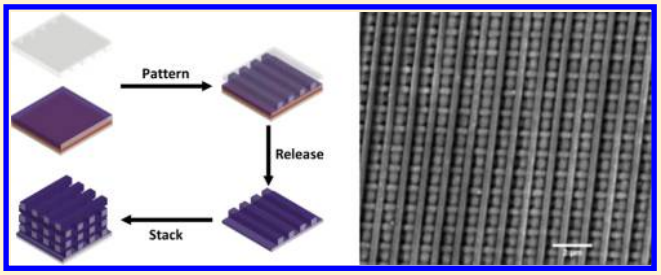

KEYWORDS: *nanoimprint lithography (NIL), nanoparticles, photonic band gap (PBG), photoresist, refractive index*

Three-dimensional photonic crystals (PCs) with a complete photonic band gap (PBG) are of broad interest to control and guide light, but their practical utility has been severely constrained by the lack of scalability using current fabrication techniques to large areas at acceptable rates and cost. Relaxation of such constraints would allow for wide-scale adoption of these materials for applications ranging from negative index metamaterials,[1,2] to ultra-low-loss waveguides,[3−5] to light extraction and spontaneous emission control,[6−9] ultimately impacting the fields of optics, optical computing, communications, and light and energy management. In general, PCs can be fabricated in one, two, or three dimensions and can exhibit a frequency gap or PBG such that certain wavelengths of electromagnetic radiation are prohibited from propagating through the PC.[10,11] Woodpile structures, or parallel arrays of orthogonally stacked rods, are the most commonly used geometry because these structures exhibit a complete PBG with a relatively low minimum refractive index (RI) contrast of approximately 1.9.[12−14]

Woodpile structures have been created using a number of techniques including holographic/interference lithography,[15−17] direct ink write,[18] and layer-by-layer micromanipulation.[9,19] Each of these techniques exhibits significant limitations such as small active areas, long processing times, high-temperature annealing steps, serial writing, or subtractive processing. Nanoimprint lithography (NIL) by contrast offers the nanometer resolution required to create PCs and is scalable by utilizing roll-to-roll (R2R) fabrication techniques, but is typically useful for producing patterns of low dimensionality and employs polymer or sol−gel resists that do not provide sufficient refractive index contrast. Several reports indicate that structures suitable for PCs can be produced directly using NIL, but optical performance is limited by the RI of the resist.[20,21] The use of conventional deposition techniques to deposit materials with the desired optical properties upon NIL-patterned media offers a solution, but such approaches lack the simplicity and scalability of direct NIL patterning. Here we describe a simple and direct patterning technique to create 3D PCs by patterning a solution-processable, hybid nanoparticle (NP)/polymer composite resist of tunable refractive index, to create grating structures followed by layering of these grating structures via a lift and stack approach to create a woodpile-type structure. Specifically, we demonstrate these methods to create a six-layer PC, with submicrometer dimensions over areas >6 cm^2 that exhibit a PBG at 840 nm. One advantage of NIL is the ease with which grating structures can be produced at dimensions ranging from a few tens of nanometers to multiple micrometers. This flexibility allows facile tuning of the PBG across broad wavelengths without sacrificing process scalability.

Received: March 16, 2014
Published: August 11, 2014

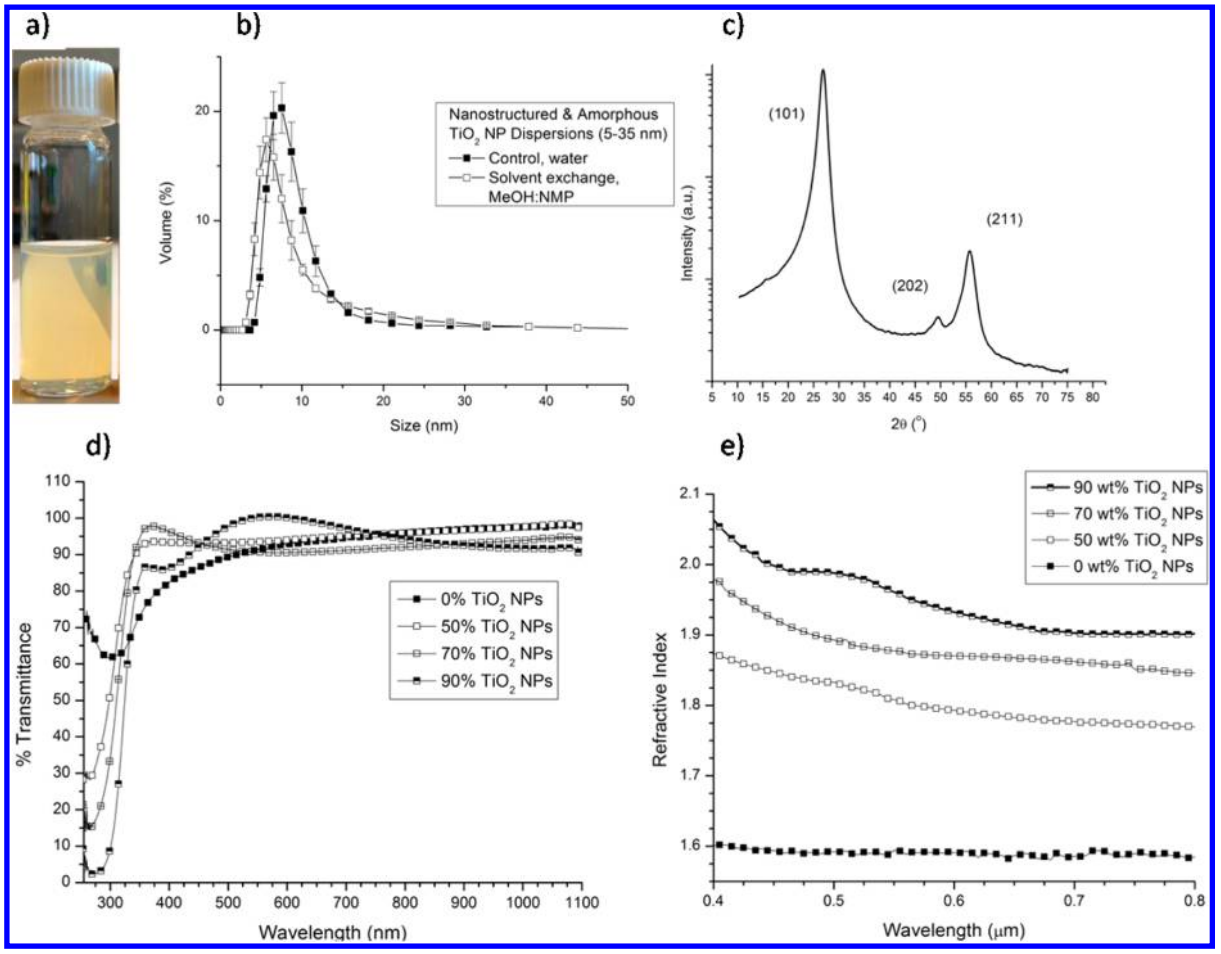

Figure 1. (a) Optical image of the solvent-exchanged TiO_2 NP dispersion. (b) Particle size distributions of the TiO_2 dispersion before and after solvent exchange. (c) X-ray diffraction data obtained after removing the solvent to obtain a TiO_2 nanopowder, showing anatase reflections. (d) UV–vis–NIR transmittance of different concentrations of TiO_2 NPs in an NOA60 photoresist. (e) Refractive index as a function of wavelength for different concentrations of TiO_2 NP.

RESULTS AND DISCUSSION

Creating PCs from patterned NP/polymer resist composites first requires the preparation of stable NP/photoresist dispersions. Even though NPs are at the forefront of nanotechnology, the solvents used to create stable NP dispersions are often limited. Most commercial NP dispersions are water-based due to electrostatic stabilization of the NPs. This reduces the compatibility of these dispersions with most imprint resists, which typically exhibit low solubility in water. To circumvent this limitation, we employ a solvent transfer technique to transfer acid-stabilized TiO_2 NPs to a mixture of *N*-methylpyrrolidone (NMP) and methanol (MeOH). We used commercially available dispersions of TiO_2 NPs of the anatase phase (RI of 2.65 at 500 nm).[22] We note that the RI is also affected by the size of the NP, such that, as the particle size is reduced, the RI is reduced as well.[23] A covalently bound NP ligand system was not employed since the ultimate RI of the composite resist would be reduced by the typically low RI of the organic ligands. Figure 1a shows an image of a translucent 5 wt % TiO_2 dispersion after solvent exchange from water into a mixture of NMP and MeOH. The particle size distribution of the TiO_2 NP dispersion before (8.6 nm) and after (8.3 nm) solvent exchange did not change, as seen in Figure 1b. These dispersions are stable for more than 12 months with negligible precipitation, which shows that these solvent-exchanged dispersions are extremely stable. Figure 1c shows X-ray diffraction analysis of recovered TiO_2 NPs, confirming the presence of anatase phase.

We used Norland optical adhesive 60 (NOA60) as a NIL photoresist since it is soluble in the NMP/MeOH solvent system and does not cause the TiO_2 NPs to aggregate after solvent evaporation, yielding transparent photoresist/NP composites, even at high NP loadings. NOA60 is sensitive to 365 nm UV light, which is important, since TiO_2 absorbs a significant amount of UV light at wavelengths below 300 nm. Straight line (0th order) optical transmittance of photo-cross-linked NP/photoresist composites is shown in Figure 1d. The film thicknesses used for the transmittance experiment ranged from 200 to 400 nm (for 0 wt % TiO_2 and 90 wt % TiO_2, respectively). A 90 wt % TiO_2 NP/photoresist composite had a transmittance value of 87% at 365 nm. Transmittance over the entire composition range of TiO_2 and NOA60 was greater than 85% for wavelengths between 400 and 1100 nm. This high transmittance shows that there was little to no aggregation present after spin coating and cross-linking the film with 365 nm UV with an energy dose of 11 J cm^{-2}.

The RI of the neat NOA60 photoresist was 1.58 at 800 nm, and the refractive index of the composite could be incrementally tuned from 1.58 up to 1.91 at 800 nm for a composite resist composed of 90 wt % TiO_2 NPs (see Figure 1e). Composite resists with TiO_2 NP concentrations above 90

dx.doi.org/10.1021/ph500078f | ACS Photonics 2014, 1, 799–805

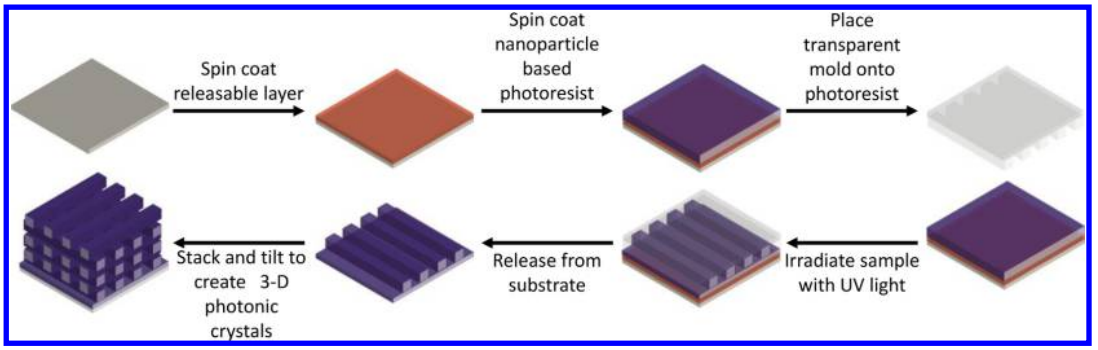

Figure 2. Patterning strategy used to generate 3D photonic crystals. First a PS/PVOH layer was spin coated in orthogonal solvents. This bilayer allows for the pattern to be released from the substrate. Next, a TiO_2 photoresist was spin coated for 15−45 s, and a transparent PDMS mold was placed on top. The samples were irradiated at 365 nm UV light with a dose of 11 J cm^{-2}. The PDMS mold was carefully peeled away from the substrate to leave behind a patterned TiO_2 NP film. Finally, the film was released from the substrate in the presence of water and stacked on a previously patterned layer.

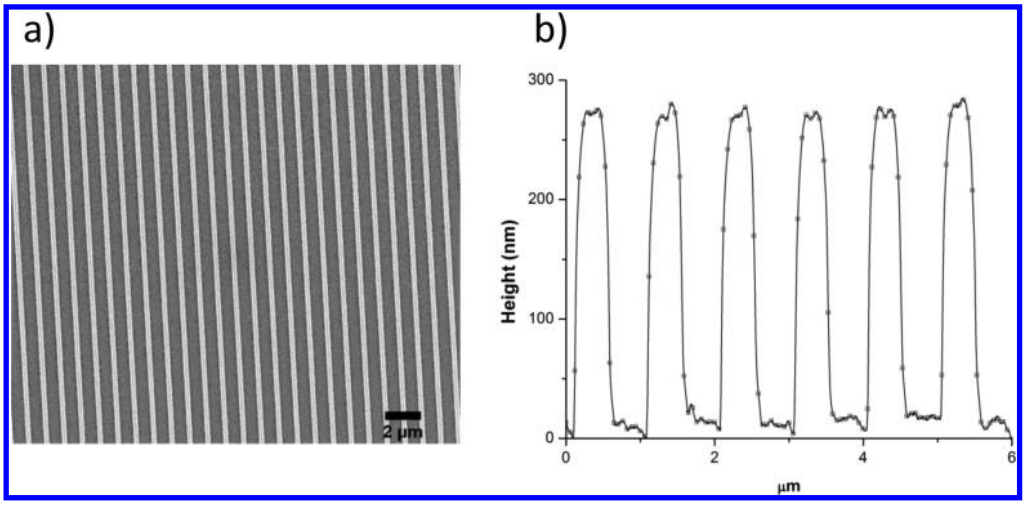

Figure 3. (a) SEM image of a 1D periodic structure (2.54 cm × 2.54 cm) composed of parallel arrays of 50 wt % TiO_2 NPs and 50 wt % NOA60. The pattern dimensions of the features were a 400 nm line width (LW) and a 1 μm pitch. (b) Height profile of representative features with a depth (D) of 300 nm.

wt % had a lower RI since this specific concentration was near the theoretical packing fraction, 64 vol % for hard spheres. Higher concentrations introduce packing frustration within the film, which effectively lowers the RI.[24]

Solvent-assisted UV-NIL, which relies upon a solvent-permeable mold, has been employed in the past to pattern NPs.[25−33] Our patterning strategy to generate PCs using solution processing of highly filled polymer/NP composites is shown in Figure 2. A TiO_2 NP/photoresist composite was spin coated onto a glass substrate, and a PDMS mold with a grating structure was brought into contact with the NP thin film. Upon contact, solvent passes through the mold, but leaves behind the NP/photoresist composite (PDMS has an NMP solvent permeability of 10.9×10^{-7} g cm s^{-1} cm^{-2}).[25] The photoresist was then cross-linked by 365 nm UV irradiation at a dose of 11 J cm^{-2}, and the mold was removed from the substrate.

Multilayer patterned structures have been demonstrated previously for metal oxides by transfer molding using water-soluble templates,[34] and 2D grating structures of CdSe nanocrystals have been prepared by microcontact molding.[35] For multilayer metal oxides, previous work requires patterning into the sol−gel precursor directly and annealing of the structures at high temperature, leading to significant shrinkage (>50%) and dimensional instability, which complicates the formation of stacked and aligned stable structures, particularly in a continuous process. The method developed in this publication was amenable to R2R NIL by stacking of the grating structures to create the PC. This required the use of a water-soluble release layer composed of poly(vinyl alcohol) (PVOH), in combination with a barrier film, poly(styrene) (PS). This bilayer was first spin coated onto the substrate, and then the TiO_2 photoresist was spin coated on top of this releasable support. The film was released over different time intervals, depending on the molecular weight of the PVOH used in the release layer, with higher molecular weights leading to longer release times. The use of PVOH with molecular weights of 6, 31, and 205 kg mol^{-1} resulted in substrate release times of 15 min, 12 h, and 3 days, respectively. PVOH with a molecular weight of 31 kg mol^{-1} was ultimately used in most of our experiments. This patterned layer of the composite resist can be picked up and stacked orthogonally to another layer, and this processing strategy can continue until the desired number of layers has been accumulated.

Figure 3a shows a top-down scanning electron microscopy (SEM) image of a 50 wt % TiO_2 patterned photoresist. We found this composition provided ease of handling for our initial experiments. A 2D height profile of the film cross-section obtained by atomic force microscopy (AFM) is shown in

dx.doi.org/10.1021/ph500078f | ACS Photonics 2014, 1, 799−805

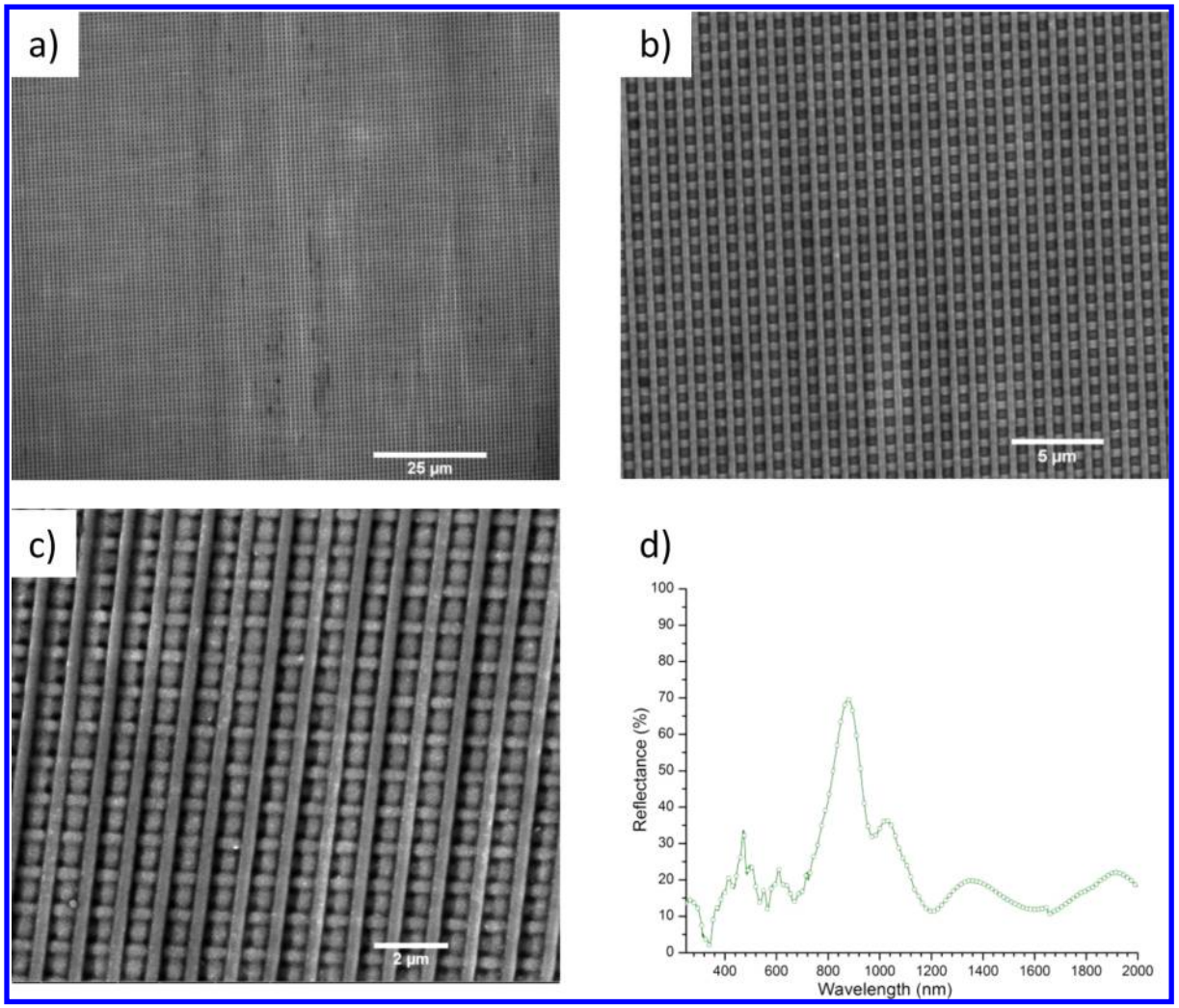

Figure 4. (a) Low-magnification top-down SEM images of a two-layer 3D photonic structure with LW = 400 nm, D = 300 nm, and P = 1.0 μm and (b) higher magnification. (c) Top-down SEM image of a four-layer 3D photonic structure and (d) UV−vis−NIR specular reflectance measurement at 35° with respect to surface normal of a six-layer 3D photonic crystal.

Figure 3b. The master mold dimensions used to generate the pattern were a 500 nm line width (LW), 500 nm depth (D), and 1000 nm pitch (P); however this technique is theoretically limited only by the NP size. Patterns with 100 nm LW and aspect ratios > 2 have been achieved in our lab with different NP resist systems, as will be reported in future publications. The pattern was created over a relatively large area (2.54 cm × 2.54 cm) with few defects. In some samples, air bubbles could be trapped between the PDMS mold and the photoresist, which was the cause of the defects. One solution was to contact the mold at one edge of the wafer and roll the mold slowly to the other edge. The dimensions of the patterned TiO_2 photoresist were slightly smaller than the master mold dimensions, 400 nm LW, 300 nm D, and 1000 nm P. This difference in pattern dimension arises from the technique used, since the solvent swells the mold during the patterning step.

A simple two-layer stack is shown in Figure 4a and b. This structure shows the degree of regularity of the PC over very large areas. The structure possesses an edge length of 2.54 cm (governed by the master mold), W = 400 nm, and P = 1000 nm. Excellent registrations between the layers is seen upon increasing the number of layers from two to four layers, Figure 4c. When the layers are increased to six layers, a maximum reflectance of 72% at 840 nm (Figure 4d) was obtained and is attributed to the regularity of the structure made by this technique. The specular reflectance measurement was 35° with respect to the sample normal. These results from a rather simple printing procedure are similar to those of log-pile TiO_2 structures fabricated using tedious, conventional top-down methods such as multilayer e-beam lithography followed by reactive ion etching.[36]

A true 3D photonic crystal should have a stop band in all directions. Despite use of a rather simple alignment procedure performed by hand, Figure 5 shows a minimum of 50% reflection over angles of incidence ranging from 25 to 65 degrees with respect to the surface normal. Improvements may be realized using feedback control for alignment. This work is under way. The magnitude of the stop-peak is due to the refractive index contrast between the composite resist and air. The refractive index of the composite resist was 1.75 at 1000 nm, which was not sufficient to create a complete PBG (n = 1.9);[12−14] however other strategies exist to enhance this refractive index contrast. The use of higher refractive index NPs in the photoresist (e.g., PbS, InSb, InP, or GaAs) is one approach that can be used to obtain a complete PBG.[37] One key advantage that the print, lift, and stack approach has over

dx.doi.org/10.1021/ph500078f | ACS Photonics 2014, 1, 799−805

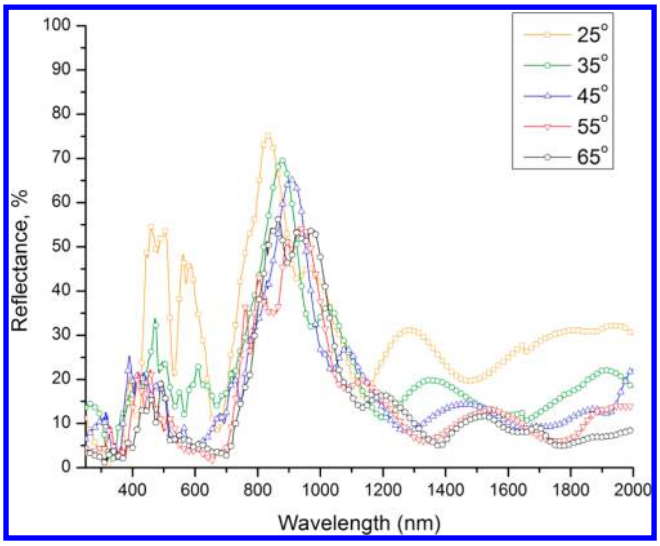

Figure 5. Angular-dependent UV−vis−NIR specular reflectance measurement (angles are denoted with respect to the surface normal) of a six-layer 3D photonic crystal.

other PC fabrication strategies is the ability to scale the technique to larger areas and higher throughputs at low cost by using R2R processing. The grating structures can be easily produced over very large areas using R2R NIL. We recently reported the large-area reproduction of nanoscale features on a moving web using this approach.[38] Stacking techniques to produce the PCs may require the use of panels or sections of the web-based gratings and feedback control or transfer printing with alignment. This is a subject of ongoing research efforts within our group. Nonetheless, a simple large-area production of gratings, and ultimately 3D PCs, has been reported here. This method offers compelling advantages relative to other techniques, which rely on high-temperature and/or serial processing steps and are significantly more difficult to scale to large areas at reasonable cost.

CONCLUSION

In conclusion, we have demonstrated an all-solution-processable strategy for generating patterned NP/NIL resist composites by solvent-assisted UV-NIL. The TiO_2 NP dispersion used for this work was solvent exchanged to enable compatibility with the photoresist. Our strategies do not require any high-temperature annealing steps, and the high-throughput nature of R2R processing, coupled with the scalability of this strategy, has the potential to enable the fabrication of inexpensive optical gratings and ultimately PBG materials over large areas.

EXPERIMENTAL SECTION

Materials. Titanium dioxide (TiO_2, anatase phase) nanoparticle (5−30 nm diameter) dispersions in water (15 wt %, Nanostructured & Amorphous Materials, Inc.), Norland optical adhesive 60 (NOA60), *N*-methyl-2-pyrrolidone (ReagentPlus 99%, Aldrich), methanol (ACS grade, Fisher Scientific), (heptadecafluoro-1,1,2,2-tetrahydrodecyl)dimethylchlorosilane (Gelest), Sylgard 184 silicone elastomer kit (polydimethylsiloxane (PDMS), Ellsworth Adhesive), 6 kg mol^{-1} poly(vinyl alcohol) (80% hydrolyzed, Polysciences, Inc.), 31 and 205 kg mol^{-1} M_w poly(vinyl alcohol) (88% hydrolyzed, Mowiol 4-88 and Mowiol 40-88, respectively, Aldrich), and 45k M_w polystyrene (Scientific Polymer Products, Inc.) were used as received without further purification. Silicon wafers of (100) orientation (p-type, boron dopant) were obtained from University Wafer. Poly(tetrafluoroethylene) (PTFE) filters (0.2 and 0.45 μm) were obtained from Fisher Scientific.

Solvent Exchange of Water-Based TiO_2 Dispersions. A 250 mL Pyrex screw-cap bottle was charged with 100 g of the TiO_2 dispersion. To this dispersion was added 100 g equal amounts (by weight) of MeOH and NMP, and the product was mixed. This solution was dried slowly with a constant flow of air for extended periods of time until the majority of the solvent was removed (greater than 50%). This dried TiO_2 NP slurry was then redispersed with the desired mixture of protic and aprotic solvents through sonication and vortex mixing. The resulting TiO_2 dispersions could have concentrations ranging from 10 wt % to 40 wt %. These organic solvent based TiO_2 NP dispersions were stable for several months.

Sylgard 184 PDMS Mold Fabrication. Master molds made from silicon were used to generate replica molds from PDMS for the solvent-assisted NIL procedure. A self-assembled monolayer (SAM) was applied to the surface of the silicon master mold to reduce the surface energy of silicon. The silicon master molds were sonicated and rinsed with water, acetone, and 2-propanol to remove any residual organic material. Then the master molds were placed in an oxygen (O_2) plasma cleaner for 15 min. The silicon molds were removed from the O_2 plasma cleaner and exposed to 1 vol %, with respect to the reactor volume, of (heptadecafluoro-1,1,2,2-tetrahydrodecyl)-dimethylchlorosilane at 80 °C for 24 h to react the silicon master mold with the SAM.

The soft, replica molds used for solvent-assisted NIL were made from Sylgard 184 PDMS, and the standard fabrication method of generating Sylgard 184 PDMS replica molds was used.[39] A 10 to 1 ratio of base to curing agent was used for the replica molds. Once the PDMS was thoroughly mixed by both hand mixing and vortexing, the mixture was degassed using a vacuum oven to remove the dissolved gases within the PDMS (note: if the mixture is placed in the vacuum oven for more than 10 min, the two components become phase separated). The degassed PDMS (20 g) was poured into 150 mm diameter PS Petri dishes containing the fluorinated silicon master molds. Then the Petri dishes were degassed for another 10 min, and the gas bubbles remaining were removed. The PDMS was cured at 75 °C for over a period of 3 h. The molds were removed from the oven and peeled away from the silicon master molds using an X-acto knife and razor blade. At this time, the PDMS replica molds were ready to be used.

All-Solution-Processable 3D Photonic Crystal. In a typical experiment, a mixture of NOA60 and solvent-exchanged TiO_2 NPs were mixed together and sonicated for 15 min prior to use. This nanocomposite photoresist was filtered through a 0.2 μm PTFE filter to remove any large particulates. Then, a silicon wafer was first spin coated with a PVOH water-soluble layer at 3000 rpm until there was no residual solvent. A PS layer was spin coated on top of this water-soluble layer to act as a barrier film, between the NP photoresist and the water-releasable layer. This substrate was placed into the spin coater in an inert atmosphere for between 5 and 15 min to reduce the humidity in the chamber prior to spin coating. Spin coating was performed for a short time, less than 30 s, at 3000 rpm, and the PDMS replica mold was placed on top of the NP composite. Capillary forces draw the mold into intimate contact with the NP composite. The patterned composite was exposed to 365

dx.doi.org/10.1021/ph500078f | ACS Photonics 2014, 1, 799−805

nm UV light with an energy of 11 J cm^{-2}. The PDMS replica mold was then peeled off uniformly to expose the underlying pattern.

Once the NP photoresist was cross-linked, it was placed into a water bath to dissolve away the water-soluble layer. When the water-soluble layer was completely dissolved, the patterned layer releases from the substrate and can be picked up with another patterned layer. The alignment between layers was performed by using a red laser (650 nm) to show the direction of the patterned lines. Once the residual water had been completely removed from the sample, the adhesion between layers was sufficient to continue to stack and tilt to generate 3D photonic crystals.

Characterization. Film thickness measurements were performed with a Veeco Dektak 150 surface profilometer, and an average of five measurements were made for the reported film thickness values. Transmittance and absorbance UV−vis−NIR measurements were performed on a Shimadzu UV-3600 UV−vis−NIR spectrophotometer. Specular reflectance measurements were performed on the same device, with a variable angle reflectance accessory in combination with a Glan Taylor polarizer from Harrick. Refractive indices were measured by variable-angle spectroscopic ellipsometry (VASE) with a Sopra GES-5 variable-angle spectroscopic ellipsometer. Modeling of the VASE data was performed with Winelli, commercial software available from Sopra, using a Cauchy-based formalism. Field emission scanning electron microscopy (FESEM) was performed on a FEI Magellan FESEM. Particle size distributions were measured by a Malvern Zetasizer 3000 HAS (Malvern Instruments Ltd., Malvern, UK) at a temperature of 25 °C and a scattering angle of 90° after diluting the NP suspension to 5 wt % solids. X-ray diffraction experiments were conducted on a PANalytical X'Pert diffractometer, using copper (Cu) Kα X-rays (0.1542 nm) operating at 45 kV and 40 mA.

AUTHOR INFORMATION

Corresponding Author

*E-mail: watkins@polysci.umass.edu.

Author Contributions

The manuscript was written through contributions of all authors.

Notes

The authors declare no competing financial interest.

ACKNOWLEDGMENTS

Funding for this research was provided by the National Science Foundation under grants CMMI-1258336 and CMMI-1025020 (Center for Hierarchical Manufacturing).

REFERENCES

(1) Cubukcu, E.; Aydin, K.; Ozbay, E.; Foteinopoulou, S.; Soukoulis, C. Subwavelength resolution in a two-dimensional photonic-crystal-based superlens. *Phys. Rev. Lett.* **2003**, *91*, 1−4.

(2) Baba, T.; Asatsuma, T.; Matsumoto, T. Negative refraction in photonic crystals. *MRS Bull.* **2011**, *33*, 927−930.

(3) Rinne, S. A.; García-Santamaría, F.; Braun, P. V. Embedded cavities and waveguides in three-dimensional silicon photonic crystals. *Nat. Photonics* **2007**, *2*, 52−56.

(4) Lin, S. Y.; Chow, E.; Johnson, S. G.; Joannopoulos, J. D. Demonstration of highly efficient waveguiding in a photonic crystal slab at the 1.5-μm wavelength. *Opt. Lett.* **2000**, *25*, 1297−1299.

(5) Bayindir, M.; Ozbay, E.; Temelkuran, B.; Sigalas, M.; Soukoulis, C.; Biswas, R.; Ho, K. Guiding, bending, and splitting of electromagnetic waves in highly confined photonic crystal waveguides. *Phys. Rev. B* **2001**, *63*, 1−4.

(6) Yoshie, T.; Scherer, A.; Hendrickson, J.; Khitrova, G.; Gibbs, H. M.; Rupper, G.; Ell, C.; Shchekin, O. B.; Deppe, D. G. Vacuum Rabi splitting with a single quantum dot in a photonic crystal nanocavity. *Nature* **2004**, *432*, 200−203.

(7) Ogawa, S.; Imada, M.; Yoshimoto, S.; Okano, M.; Noda, S. Control of light emission by 3D photonic crystals. *Science* **2004**, *305*, 227−229.

(8) Lodahl, P.; Driel, A. F.; Van Nikolaev, I. S.; Irman, A.; Overgaag, K.; Vanmaekelbergh, D.; Vos, W. L. Controlling the dynamics of spontaneous emission from quantum dots by photonic crystals. *Nature* **2004**, *430*, 654−657.

(9) Aoki, K.; Guimard, D.; Nishioka, M.; Nomura, M.; Iwamoto, S.; Arakawa, Y. Coupling of quantum-dot light emission with a three-dimensional photonic-crystal nanocavity. *Nat. Photonics* **2008**, *2*, 688−692.

(10) Yablonovitch, E. Inhibited spontaneous emission in solid-state physics and electronics. *Phys. Rev, Lett.* **1987**, *58*, 2059−2062.

(11) John, S. Strong localization of photons in certain disordered dielectric superlattices. *Phys. Rev. Lett.* **1987**, *58*, 2486−2489.

(12) Park, S.-G.; Miyake, M.; Yang, S.-M.; Braun, P. V. Cu_2O inverse woodpile photonic crystals by prism holographic lithography and electrodeposition. *Adv. Mater.* **2011**, *23*, 2749−2752.

(13) Ozbay, E.; Abeyta, A.; Tuttle, G.; Tringides, M.; Biswas, R.; Chan, C. T.; Soukoulis, C. M.; Ho, K. M. Measurement of a three-dimensional photonic band gap in a crystal structure made of dielectric rods. *Phys. Rev. B* **1994**, *50*, 1945−1949.

(14) Ho, K. M.; Chan, C. T.; Soukoulis, C. M.; Biswas, R.; Sigalas, M. Photonic band gaps in three dimensions: New layer-by-layer periodic structures. *Solid State Commun.* **1994**, *89*, 413.

(15) Campbell, M.; Sharp, D. N.; Harrison, M. T.; Denning, R. G. Fabrication of photonic crystals for the visible spectrum by holographic lithography. *Nature* **2000**, *404*, 53−56.

(16) Shoji, S.; Kawata, S. Photofabrication of three-dimensional photonic crystals by multibeam laser interference into a photopolymerizable resin. *Appl. Phys. Lett.* **2000**, *76*, 2668.

(17) Miklyaev, Y. V.; Meisel, D. C.; Blanco, A.; Von Freymann, G.; Busch, K.; Koch, W.; Enkrich, C.; Deubel, M.; Wegener, M. Three-dimensional face-centered-cubic photonic crystal templates by laser holography: fabrication, optical characterization, and band-structure calculations. *Appl. Phys. Lett.* **2003**, *82*, 1284.

(18) Duoss, E. B.; Twardowski, M.; Lewis, J. A. Sol-gel inks for direct-write assembly of functional oxides. *Adv. Mater.* **2007**, *19*, 3485−3489.

(19) Aoki, K.; Miyazaki, H. T.; Hirayama, H.; Inoshita, K.; Baba, T.; Sakoda, K.; Shinya, N.; Aoyagi, Y. Microassembly of semiconductor three-dimensional photonic crystals. *Nat. Mater.* **2003**, *2*, 117−121.

(20) Glinsner, T.; Lindner, P.; Mühlberger, M.; Bergmair, I.; Schöftner, R.; Hingerl, K.; Schmid, H.; Kley, E.-B. Fabrication of 3D-photonic crystals via UV-nanoimprint lithography. *J. Vac. Sci. Technol. B* **2007**, *25*, 2337.

(21) Verschuuren, M.; van Sprang, H. 3D photonic structures by sol-gel imprint lithography. *MRS Symp. Proc.* **2007**, *1002*, 1−6.

(22) King, J. S.; Graugnard, E.; Summers, C. J. TiO_2 inverse opals fabricated using low-temperature atomic layer deposition. *Adv. Mater.* **2005**, *17*, 1010−1013.

(23) Geethalakshmi, K.; Prabhakaran, T.; Hemalatha, J. Dielectric studies on nano zirconium dioxide synthesized through co-precipitation process. *World Acad. Sci. Eng. Technol.* **2012**, *64*, 179−182.

(24) Farr, R. S.; Groot, R. D. Close packing density of polydisperse hard spheres. *J. Chem. Phys.* **2009**, *131*, 244104.

(25) Demko, M. T.; Cheng, J. C.; Pisano, A. P. Rigid, vapor-permeable poly(4-methyl-2-pentyne) templates for high resolution patterning of nanoparticles and polymers. *ACS Appl. Mater. Interfaces* **2012**, *6*, 6890−6896.

(26) Kim, E.; Xia, Y.; Whitesides, G. M. Polymer microstructures formed by molding in capillaries. *Nature* **1995**, *376*, 581−584.
(27) Kim, E.; Xia, Y.; Zhao, X.; Whitesides, G. M. Solvent-assisted microcontact molding: a convenient method for fabricating three-dimensional structures on surfaces of polymers. *Adv. Mater.* **1997**, *9*, 651−654.
(28) Lee, M. H.; Huntington, M. D.; Zhou, W.; Yang, J.; Odom, T. W. Programmable soft lithography: solvent-assisted nanoscale embossing. *Nano Lett.* **2011**, *11*, 311−315.
(29) Kim, Y. S.; Suh, K. Y.; Lee, H. H. Fabrication of three-dimensional microstructures by soft molding. *Appl. Phys. Lett.* **2001**, *79*, 2285.
(30) Demko, M. T.; Cheng, J. C.; Pisano, A. P. High-resolution direct patterning of gold nanoparticles by the microfluidic molding process. *Langmuir* **2010**, *26*, 16710−16714.
(31) Demko, M. T.; Brackbill, T. P.; Pisano, A. P. Simultaneous patterning of nanoparticles and polymers using an evaporation driven flow in a vapor permeable template. *Langmuir* **2012**, *28*, 9857−9863.
(32) Liu, C. H.; Sung, C. K.; Chang, E. C.; Lo, C. Y.; Fu, C. C. Fabricating a silver soft mold on a flexible substrate for roll-to-roll nanoimprinting. *IEEE Trans. Nanotechnol.* **2014**, *13*, 80−84.
(33) Kim, E. U.; Baeg, K. J.; Noh, Y. Y.; Kim, D. Y.; Lee, T.; Park, I.; Jung, G. Y. Templated assembly of metal nanoparticles in nano-imprinted patterns for metal nanowire fabrication. *Nanotechnology* **2009**, *20*, 355302−355308.
(34) Bass, J. D.; Schaper, C. D.; Rettner, C. T.; Arellano, N.; Alharbi, F. H.; Miller, R. D.; Kim, H. Transfer molding of nanoscale oxides using water-soluble templates. *ACS Nano* **2011**, *5*, 4065−4072.
(35) Shallcross, R. C.; Chawla, G. S.; Marikkar, F. S.; Tolbert, S.; Pyun, J.; Armstrong, N. R. Efficient CdSe nanocrystal diffraction gratings prepared by microcontact molding. *ACS Nano* **2009**, *3*, 3629−3637.
(36) Subramania, G.; Lee, Y.-J.; Fischer, A. J.; Koleske, D. D. Log-pile TiO_2 photonic crystal for light control at near-UV and visible wavelengths. *Adv. Mater.* **2010**, *22*, 487−491.
(37) Weibel, M.; Caseri, W.; Suter, U. W.; Kiess, H.; Wehrli, E. Preparation of polymer nanocomposites with "ultrahigh" refractive index. *Polym. Adv. Technol.* **1991**, *2*, 75−80.
(38) John, J.; Tang, Y.; Rothstein, J. P.; Watkins, J. J.; Carter, K. R. Large-area, continuous roll-to-roll nanoimprinting with PFPE composite molds. *Nanotechnology* **2013**, *24*, 505307.
(39) Moran, I. W.; Briseno, A. L.; Loser, S.; Carter, K. R. Device fabrication by easy soft imprint nano-lithography. *Chem. Mater.* **2008**, *20*, 4595−4601.